

Diphenoxo-bridged NiCo and CuCo complexes of macrocyclic ligands: synthesis, structure and electrochemical behaviour †

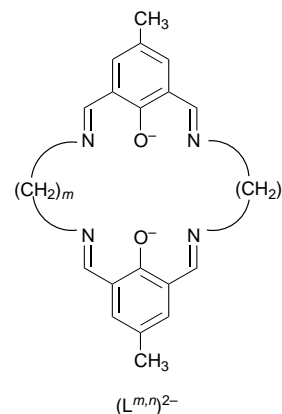
Takanori Aono, Hisae Wada, Masami Yonemura, Hideki Furutachi, Masaaki Ohba and Hisashi Ōkawa *

Department of Chemistry, Faculty of Science, Kyushu University, Hakozaki 6-10-1, Higashiku, Fukuoka 812, Japan

Heterodinuclear di- μ -phenoxo- $M^I M^II$ ($M = \text{Ni}$ or Cu) complexes have been derived from phenol-based dinucleating ligands $(L^{m,n})^{2-}$, comprising of two 2,6-di(iminomethyl)-4-methylphenolate entities linked by two lateral chains $(\text{CH}_2)_m$ ($m = 2$ or 3) and $(\text{CH}_2)_n$ ($n = 3$ or 4) at the imino nitrogens. The crystal structure of $[\text{CuCo}(L^{2,3})(\text{dmf})_2(\text{H}_2\text{O})][\text{ClO}_4]_2$ ($\text{dmf} = \text{dimethylformamide}$) has been determined. The copper ion resides at the N_2O_2 site formed by the ethylene lateral chain and assumes a square-pyramidal geometry together with a dmf oxygen at the apex. The Co at the site of the trimethylene lateral chain assumes a pseudo-octahedral geometry together with a dmf and a water molecule at the axial positions. The $\text{Cu} \cdots \text{Co}$ separation doubly bridged by the phenolic oxygens is $2.998(2)$ Å. The NiCo complexes are paramagnetic ($S_{\text{Ni}} = 0$), whereas the CuCo complexes show a strong antiferromagnetic interaction between the two metal ions. Cyclic voltammograms of the NiCo complexes show two quasi-reversible couples attributable to the stepwise reductions: $\text{Ni}^II \text{Co}^II \longrightarrow \text{Ni}^I \text{Co}^II \longrightarrow \text{Ni}^I \text{Co}^I$. The $\text{Ni}^I \text{Co}^II$ and $\text{Ni}^I \text{Co}^I$ complexes were prepared in solution by coulometry and characterized by visible spectroscopy. Similarly, the CuCo complex of $(L^{3,3})^{2-}$ is reduced stepwise to $\text{Cu}^I \text{Co}^II$ and then to $\text{Cu}^I \text{Co}^I$. On the other hand, the CuCo complexes of $(L^{2,3})^{2-}$ and $(L^{2,4})^{2-}$ showed unusual electrochemical behaviour at the electrode suggesting a scrambling or site exchange of the metal ions.

Heterodinuclear metal complexes are of current interest because of their properties and functions arising from interactions or co-operative functions of a pair of dissimilar metal ions in close proximity.¹⁻³ Recently heterodinuclear cores have been recognized at metallobsites of purple acid phosphatase (FeZn),⁴ human calcineurin (FeZn)⁵ and human protein phosphatase 1 (MnFe)⁶ and these findings have stimulated interest in heterodinuclear metal complexes. With the aim of providing discrete heterodinuclear core complexes, compartmental ligands of various types have been developed the two metal-binding sites of which are not equivalent with respect to cavity size, co-ordination number, or nature of donor atom.⁷ Phenol-based dinucleating macrocycles having two non-equivalent metal-binding sites⁸⁻¹⁴ are of particular value for the study of heterodinuclear complexes because the resulting di- μ -phenoxo- $M^I M^II$ core complexes are thermodynamically stabilized by the macrocyclic effect and the core structures can be tuned by modification of the macrocycles. Further, we have noticed that unusual oxidation states of heterodinuclear cores can be stabilized by the use of macrocyclic ligands. Such unusual oxidation states have been little studied so far in spite of great interest in their electronic structure, properties and functions.

In this study heterodinuclear $\text{Ni}^II \text{Co}^II$ and $\text{Cu}^II \text{Co}^II$ complexes have been derived from the phenol-based macrocycles $(L^{m,n})^{2-}$,^{8,9,15} $m, n = (2,3), (2,4)$ or $(3,3)$ where the superscripts m and n denote the numbers of methylene groups of the two lateral chains. X-Ray crystallography for $[\text{CuCo}(L^{2,3})(\text{dmf})_2(\text{H}_2\text{O})][\text{ClO}_4]_2$ ($\text{dmf} = \text{dimethylformamide}$) confirmed a discrete heterodinuclear core structure having the Cu at the N_2O_2 site of the ethylene lateral chain (square-pyramidal with one dmf oxygen at the apical site) and the Co at the site of the trimethylene lateral chain (pseudo-octahedral with one water and one dmf oxygen at the apical sites). Emphasis is placed on electrochemical property of the complexes to provide $M^I \text{Co}^II$ and $M^I \text{Co}^I$ ($M = \text{Ni}$ or



Cu) species or to cause a scrambling or site exchange of metal ions depending upon the combination of metal ions and the m, n set of the lateral chains of $(L^{m,n})^{2-}$.

Experimental

Measurements

Elemental analyses of C, H, and N were obtained at the Elemental Analysis Service Center of Kyushu University. Metal analyses were made using a Shimadzu AA-680 atomic absorption/flame emission spectrophotometer. Infrared spectra were recorded on a JASCO IR-810 spectrometer using KBr discs. Molar conductances were measured on a DKK AOL-10 conductivity meter in dimethyl sulfoxide (dmsO) at 20°C at $\approx 1 \times 10^{-3}$ M. Electronic absorption spectra were recorded on a Shimadzu MPS-2000 spectrometer. Magnetic susceptibilities were determined on a Faraday balance in the temperature range $80\text{--}300$ K and on a HOXAN HSM-D SQUID susceptometer in the range $4.2\text{--}80$ K. Calibrations were made using $[\text{Ni}(\text{en})_3][\text{S}_2\text{O}_3]^{16}$ ($\text{en} = \text{ethane-1,2-diamine}$) and diamagnetic corrections were made using Pascal's constants.¹⁷ Cyclic voltammograms

† Non-SI unit employed: $\mu_B \approx 9.27 \times 10^{-24}$ J T⁻¹.

were measured using a BAS CV-50W electrochemical analyzer in dmsO solution containing tetra(*n*-butyl)ammonium perchlorate as the supporting electrolyte (**CAUTION**: this compound is explosive and should be handled with great care). A three-electrode cell was used which was equipped with a glassy-carbon working electrode, a platinum coil as the counter electrode, and a Ag–Ag⁺ (NBu₄⁺ClO₄⁻-acetonitrile) reference electrode. Controlled-potential electrolyses were made on an apparatus comprising a HA-501 potentiostat/galvanostat, a HB-104 function generator, and a HF-201 coulomb/amperehour meter from Hokuto Denko Ltd. X-Band ESR spectra were recorded using a JEOL JEX-FE3X spectrometer at liquid-nitrogen temperature.

Materials

2,6-Diformyl-4-methylphenol was prepared by the method of Denton and Suschitzky.¹⁸ Trinuclear [Pb{M(L^{*m,n*})₂}]₂[ClO₄]₂ [M = Ni or Cu; *m,n* = (2,3), (2,4) or (3,3)] were synthesized by the literature method.⁹ All the other chemicals were of reagent grade and used as received.

Preparations

[NiCo(L^{2,3})]₂[ClO₄]₂·H₂O **1.** A solution of cobalt(II) perchlorate hexahydrate (92 mg, 0.25 mmol) and cobalt(II) sulfate heptahydrate (70 mg, 0.25 mmol) in methanol (10 cm³) was added to a suspension of [Pb{Ni(L^{2,3})₂}]₂[ClO₄]₂·2H₂O (324 mg, 0.25 mmol) in acetonitrile (20 cm³), and the mixture was stirred at ambient temperature for 3 h. The resulting precipitate (PbSO₄) was filtered off and the filtrate evaporated to dryness. The residue was extracted with acetonitrile and the extract filtered to separate PbSO₄. This operation (dissolution in acetonitrile and then filtration to separate PbSO₄) was repeated until PbSO₄ no longer appeared. The crude product was dissolved in acetonitrile and the solution diffused with diethyl ether to give red microcrystals. Yield 240 mg (65%) (Found: C, 38.31; H, 3.65; Co, 7.7; N, 7.75; Ni, 8.3. Calc. for C₂₃H₂₆Cl₂CoNi₄NiO₁₁: C, 38.21; H, 3.63; Co, 8.2; N, 7.75; Ni, 8.1%). Selected IR (KBr): 2920, 1630, 1560, 1320, 1100 and 620 cm⁻¹. UV/VIS [λ_{\max} /nm ($\epsilon/M^{-1} \text{ cm}^{-1}$)] in dmsO: 390 (9500) and 520 (sh). Conductance ($\Lambda_M/S \text{ cm}^2 \text{ mol}^{-1}$) in dmsO: 60.

[NiCo(L^{2,4})]₂[ClO₄]₂·H₂O **2.** This complex was synthesized in a similar way to that for **1**, except for the use of [Pb{Ni(L^{2,4})₂}]₂[ClO₄]₂·H₂O instead of [Pb{Ni(L^{2,3})₂}]₂[ClO₄]₂·2H₂O. Yield 240 mg (65%) (Found: C, 39.19; H, 3.86; Co, 7.7; N, 7.72; Ni, 7.9. Calc. for C₂₄H₂₈Cl₂CoNi₄NiO₁₁: C, 39.11; H, 3.83; Co, 8.0; N, 7.60; Ni, 8.0%). Selected IR (KBr): 2910, 1630, 1560, 1320, 1100 and 620 cm⁻¹. UV/VIS [λ_{\max} /nm ($\epsilon/M^{-1} \text{ cm}^{-1}$)] in dmsO: 390 (9300) and 520 (sh). Conductance ($\Lambda_M/S \text{ cm}^2 \text{ mol}^{-1}$) in dmsO: 60.

[CuCo(L^{2,3})]₂[ClO₄]₂ **3.** This complex was prepared in a similar way to that for **1**, by the reaction of [Pb{Cu(L^{2,3})₂}]₂[ClO₄]₂ (323 mg, 0.25 mmol) with cobalt(II) perchlorate hexahydrate (92 mg, 0.25 mmol) and cobalt(II) sulfate heptahydrate (70 mg, 0.25 mmol). The crude product was dissolved in dry methanol and the solution diffused with ether to give brown microcrystals. Yield 280 mg (77%) (Found: C, 37.91; H, 3.53; Co, 7.8; Cu, 8.9; N, 7.72. Calc. for C₂₃H₂₆Cl₂CoCuN₄O₁₁: C, 37.95; H, 3.60; Co, 8.1; Cu, 8.7; N, 7.70%). Selected IR (KBr): 2910, 1630, 1560, 1320, 1100 and 620 cm⁻¹. UV/VIS [λ_{\max} /nm ($\epsilon/M^{-1} \text{ cm}^{-1}$)] in dmsO: 370 (12 000) and 550 (200). Conductance ($\Lambda_M/S \text{ cm}^2 \text{ mol}^{-1}$) in dmsO: 60.

A portion was dissolved in dmF and the solution layered with ether to give good single crystals of [CuCo(L^{2,3})-(dmF)₂(H₂O)]₂[ClO₄]₂ **3'** suitable for X-ray crystallography (Found: C, 39.89; H, 4.68; Co, 6.8; Cu, 7.4; N, 9.65. Calc. for C₂₉H₄₀Cl₂CoCuN₆O₁₃: C, 39.85; H, 4.61; Co, 6.7; Cu, 7.3; N, 9.62%).

[CuCo(L^{2,4})]₂[ClO₄]₂·H₂O **4.** This was obtained as brown microcrystals using [Pb{Cu(L^{2,4})₂}]₂[ClO₄]₂ instead of [Pb{Cu(L^{2,3})₂}]₂[ClO₄]₂. Yield 285 mg (70%) (Found: C, 38.98; H, 3.84; Co, 8.4; Cu, 9.0; N, 7.60. Calc. for C₂₄H₂₈Cl₂CoCuN₄O₁₁: C, 38.86; H, 3.80; Co, 7.9; Cu, 8.6; N, 7.55%). Selected IR (KBr): 2910, 1640, 1550, 1320, 1100 and 620 cm⁻¹. UV/VIS [λ_{\max} /nm ($\epsilon/M^{-1} \text{ cm}^{-1}$)] in dmsO: 370 (12 000) and 550 (180). Conductance ($\Lambda_M/S \text{ cm}^2 \text{ mol}^{-1}$) in dmsO: 61.

[CuCo(L^{3,3})]₂[ClO₄]₂·CH₃OH **5.** This was obtained as deep green microcrystals using [Pb{Cu(L^{3,3})₂}]₂[ClO₄]₂-dmF. Yield 260 mg (72%) (Found: C, 39.57; H, 3.95; Co, 7.9; Cu, 8.7; N, 7.44. Calc. for C₂₄H₂₈Cl₂CoCuN₄O₁₁: C, 39.72; H, 4.00; Co, 7.8; Cu, 8.5; N, 7.41%). Selected IR (KBr): 2920, 1630, 1560, 1320, 1100 and 620 cm⁻¹. UV/VIS [λ_{\max} /nm ($\epsilon/M^{-1} \text{ cm}^{-1}$)] in dmsO: 370 (14 000), 550 (150) and 620 (140). Conductance ($\Lambda_M/S \text{ cm}^2 \text{ mol}^{-1}$) in dmsO: 61.

Crystallography

A single crystal (0.20 × 0.20 × 0.30 mm) of [CuCo(L^{2,3})(dmF)₂(H₂O)]₂[ClO₄]₂ **3'** was used for data collection on a Rigaku AFC7R four-circle diffractometer, using graphite-monochromated Mo-K α radiation ($\lambda = 0.710 69 \text{ \AA}$) and a 12 kW rotating-anode generator at 293 K. Cell constants and an orientation matrix for data collection were obtained from 25 reflections in the range 22.43 < 2 θ < 29.73°. For the intensity collections the ω -2 θ scan mode was used to a maximum 2 θ value of 16.0° min⁻¹. The octant measured was +*h*, +*k*, +*l* (0 to 18, 0 to 19, 0 to 18). Pertinent crystallographic parameters are summarized in Table 1. A total of 3721 reflections was collected. Three standard reflections were monitored every 150 measurements. Over the course of the data collection the standards decreased by 6.6%. A linear correction factor was applied to the data to account for this. The linear absorption coefficient, μ , for Mo-K α radiation was 12.24 cm⁻¹. Azimuthal scans of several reflections indicated no need for an absorption correction. Reflection data were corrected for Lorentz-polarization effects.

The structure was solved by the direct method and refined by Fourier techniques. The function minimized was $\sum w(|F_o| - |F_c|)^2$ with $w = 1/\sigma^2(F_o)$. Non-hydrogen atoms were anisotropically refined. Hydrogen atoms were included in the structure-factor calculations but not refined. The final cycle of full-matrix least-squares refinement was based on 2673 observed reflections with $I > 3.00\sigma(I)$ and converged with $R = 0.043$ and $R' = 0.038$. The unweighted and weighted factors were defined as $R = \sum ||F_o| - |F_c||/\sum |F_o|$ and $R' = [\sum w(|F_o| - |F_c|)^2/\sum w|F_o|^2]^{1/2}$. Neutral atom scattering factors were taken from Cromer and Waber.¹⁹ Anomalous dispersion effects were included in the final calculations; the values for $\Delta f'$ and $\Delta f''$ were those of Creagh and McAuley.²⁰ The values for the mass attenuation coefficients were those of Creagh and Hubbell.²¹ All calculations were performed using the TEXSAN crystallographic software package.²²

CCDC reference number 186/629.

Results and Discussion

Synthesis and general properties

The macrocycles (L^{*m,n*})²⁻ have been obtained by the stepwise template reaction devised in our laboratory as trinuclear [Pb{M(L^{*m,n*})₂}]₂[ClO₄]₂ [M = Ni or Cu; *m,n* = (2,3), (2,4) or (3,3)].⁹ They were used as the precursors for the Ni^{II}Co^{II} **1,2** and Cu^{II}Co^{II} **3-5** complexes in this study. The transmetalation was successfully achieved when [Pb{M(L^{*m,n*})₂}]₂[ClO₄]₂, a metal(II) perchlorate salt and a metal(II) sulfate salt were allowed to react in the 1 : 1 : 1 stoichiometry in an appropriate solvent. The complexes **1-5** are new though a CuCo chloride complex of (L^{3,3})²⁻ was reported previously.^{23,24}

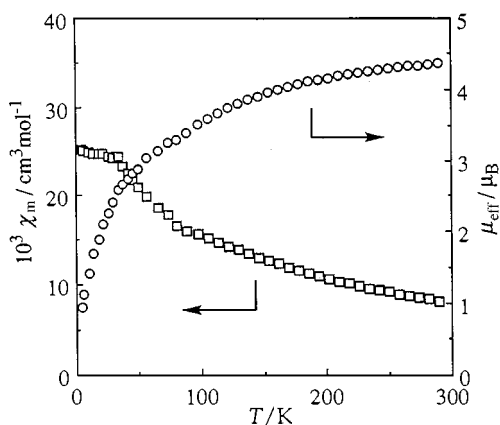


Fig. 1 Plots of μ_{eff} vs. T and χ_m vs. T for complex **3**

The complexes show an intense absorption band at 370–390 nm in dmsO that is assigned to the π - π^* transition of the azomethine linkage.^{24,25} A weak absorption near 520 nm found for the NiCo complexes **1** and **2** is assigned to the superposed d-d band of the planar nickel(II) ion.²⁵ The CuCo complexes **3** and **4** show a well resolved absorption band near 550 nm that is assigned to a superposed d-d band of the Cu^{II}.^{26,27} The d-d bands due to Co^{II} are not resolved for all the complexes. The CuCo complex **5** shows two visible bands at 565 and 620 nm²⁴ that can be assigned to d-d components of the copper(II) ion. All the complexes function as 2 : 1 electrolytes in dmsO ($\Lambda_M \approx 60 \text{ S cm}^{-2} \text{ mol}^{-1}$).

The room-temperature magnetic moments of complexes **1** and **2** are 5.00 and 4.74 μ_B (per molecule), respectively, which are common for high-spin Co^{II}. Evidently the nickel(II) ion in these complexes is diamagnetic.

The CuCo complexes **3–5** have similar cryomagnetic properties. The χ_m vs. T and μ_{eff} vs. T curves of **3** are given in Fig. 1. The μ_{eff} vs. T curve shows a near plateau (3.3 μ_B) around 90 K; the moment corresponds to the value for $S=1$ arising from the coupling of $S_{\text{Cu}} = \frac{1}{2}$ and $S_{\text{Co}} = \frac{3}{2}$. This is taken as evidence for strong antiferromagnetic interaction between the copper(II) and cobalt(II) ions. Below 80 K the magnetic moment further decreases with decreasing temperature to 0.95 μ_B at liquid-helium temperature. A similar drop in magnetic moment at low temperature is also seen for **4** and **5**. This fact suggests that a significant secondary effect operates in these complexes. A strong antiferromagnetic spin exchange ($-J > 22 \text{ cm}^{-1}$) is inferred between the copper(II) and cobalt(II) ions from the μ_{eff} vs. T curve in the range of 80–300 K, but magnetic simulations were not made in this study.

Crystal structure of $[\text{CuCo}(\text{L}^{2,3})(\text{dmf})_2(\text{H}_2\text{O})][\text{ClO}_4]_2 \mathbf{3}'$

An ORTEP²⁸ drawing of the complex is shown in Fig. 2 together with the numbering scheme. Selected bond distances and angles are given in Table 2. The complex cation is composed of $(\text{L}^{2,3})^{2-}$, one copper(II) ion, one cobalt(II) ion, two dmf molecules and one water molecule. Two perchlorate ions are free from co-ordination and captured in the crystal lattice. This is in accord with no split ν_3 mode of the perchlorate group. The $\text{CuCo}(\text{L}^{2,3})^{2+}$ entity, except for the axial donor groups (dmf and water), forms a near coplane. The Cu^{II} resides at the N_2O_2 site with the ethylene lateral chain and assumes a square-pyramidal geometry together with the dmf oxygen [O(5)] at the axial site. The in-plane Cu–N(1), Cu–N(2), Cu–O(1) and Cu–O(2) bond distances range from 1.903(7) Å to 1.908(6) Å. The axial Cu–O(5) (dmf) bond [2.658(6) Å] is elongated owing to the Jahn–Teller effect of d^9 electronic configuration of Cu^{II}. The deviation of Cu from the basal least-squares plane towards O(5) is small (0.047 Å).

The Co^{II} resides at the N_2O_2 site of the trimethylene lateral chain and assumes a pseudo-octahedral geometry together with

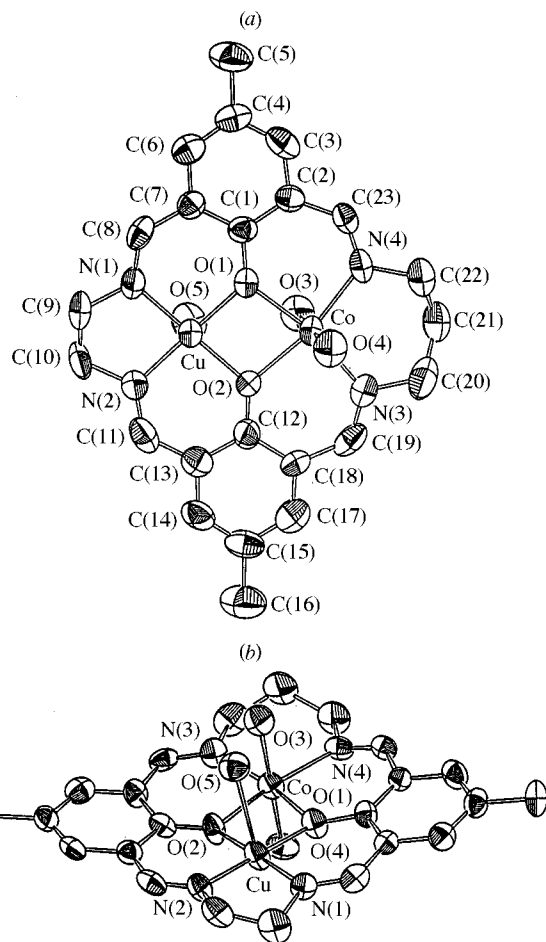


Fig. 2 An ORTEP view of $[\text{CuCo}(\text{L}^{2,3})(\text{dmf})_2(\text{H}_2\text{O})][\text{ClO}_4]_2 \mathbf{3}'$: (a) top view and (b) side view

Table 1 Crystallographic parameters for $[\text{CuCo}(\text{L}^{2,3})(\text{dmf})_2(\text{H}_2\text{O})][\text{ClO}_4]_2 \mathbf{3}'$

| | |
|--|--|
| Formula | $\text{C}_{29}\text{H}_{40}\text{Cl}_2\text{CoCuN}_6\text{O}_{13}$ |
| Colour of crystal | Reddish brown |
| M | 874.05 |
| Crystal system | Orthorhombic |
| Space group | $P2_12_12_1$ (no. 19) |
| $a/\text{\AA}$ | 15.508(8) |
| $b/\text{\AA}$ | 16.256(9) |
| $c/\text{\AA}$ | 14.838(7) |
| $UV/\text{\AA}^3$ | 3740(2) |
| Z | 4 |
| $D_c/\text{g cm}^{-3}$ | 1.552 |
| No. reflections with $ F_o \geq 3\sigma(F_o)$ | 2673 |
| $R(000)$ | 1800 |
| R | 0.043 |
| R' | 0.038 |

the water oxygen O(3) and dmf oxygen O(4) at the axial positions. The dmf molecules attached to the Cu^{II} and the Co^{II} are *trans* to each other with respect to the molecular coplane. The in-plane Co–N(3), Co–N(4), Co–O(1) and Co–O(2) bond lengths fall in the range 2.027(7)–2.047(5) Å which are longer than those in the copper chromophore. The axial Co–O(3) (water) and Co–O(4) (dmf) bonds are elongated [2.189(6) and 2.142(6) Å, respectively]. The Co^{II} is 0.059 Å from the basal least-squares plane towards O(4). The Cu \cdots Co intermetallic separation is 2.998(2) Å and the Cu–O(1)–Co and Cu–O(2)–Co angles are 99.0(2) and 98.7(2)°, respectively.

It is to be noted that the corresponding Cu^{II}Mn^{II} and Ni^{II}–Mn^{II} complexes²⁹ show a large deviation of the Mn^{II} from the basal N_2O_2 plane, giving a six-co-ordinate geometry together

Table 2 Selected bond distances (Å) and angles (°) of [CuCo(L^{2,3})-(dmf)₂(H₂O)][ClO₄]₂ **3'**

| | | | |
|--------------|----------|--------------|----------|
| Cu–O(1) | 2.033(5) | Cu–O(1) | 1.907(5) |
| Cu–O(2) | 2.047(5) | Cu–O(2) | 1.903(7) |
| Co–N(3) | 2.027(7) | Cu–N(1) | 1.908(6) |
| Co–N(4) | 2.043(7) | Cu–N(2) | 1.903(7) |
| Co–O(3) | 2.189(6) | Cu–O(5) | 2.658(6) |
| Co–O(4) | 2.142(6) | Cu···Co | 2.998(2) |
| | | | |
| Cu–O(1)–Co | 99.0(2) | O(1)–Co–O(2) | 77.5(2) |
| Cu–O(2)–Co | 98.7(2) | N(3)–Co–N(4) | 102.6(3) |
| O(1)–Cu–O(2) | 84.2(2) | O(1)–Co–N(4) | 89.7(2) |
| N(1)–Cu–N(2) | 86.8(3) | O(2)–Co–N(3) | 90.0(2) |
| O(1)–Cu–N(1) | 94.1(2) | | |
| O(2)–Cu–N(2) | 94.8(3) | | |

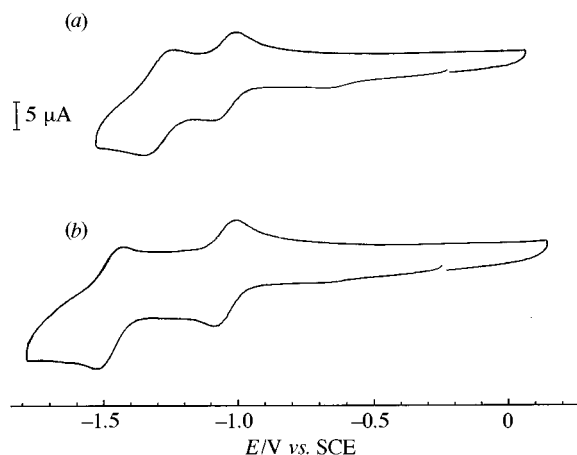


Fig. 3 Cyclic voltammograms of (a) complex **1** and (b) **2**. Conditions: glassy-carbon electrode, scan rate 50 mV s⁻¹, concentration 1 × 10⁻³ M, in dmsO

with two dmf molecules in *cis* positions. The corresponding Mn^{II}Mn^{II} complexes also have a similar large deviation of the Mn where a bidentate acetate group occupies two positions.³⁰ Such a deviation of Mn^{II} from the N₂O₂ cavity arises from the mismatch between the cavity size and the large ionic radius of Mn^{II} (0.96 Å). Cobalt(II) has a smaller ionic radius (0.88 Å for six-co-ordination) so it can be accommodated within the N₂O₂ cavity of the macrocycles.

Electrochemical behaviour and M^ICo^{II} and M^ICo^I (M = Ni or Cu) complexes

The electrochemical properties of complexes **1–5** were studied by means of cyclic voltammetry in dmsO for reduction and in acetonitrile for oxidation. Our attention was focused on the reduction waves of the complexes because cyclic voltammograms in the positive potential region were ill resolved.

Cyclic voltammograms of the NiCo complexes **1** and **2** are given in Fig. 3. Complex **1** shows two quasi-reversible couples at -1.00 and -1.25 V (*vs.* saturated calomel electrode, SCE). Similarly, **2** exhibits two quasi-reversible couples at -1.02 and -1.44 V. The first wave near -1.0 V is attributed to the reduction of the nickel(II) centre based on coulometry for **2** at -1.05 V. The electrolysed solution is deep green and shows three intense absorption bands at 560 (1100), 630 (1100) and 820 nm ($\epsilon = 500 \text{ M}^{-1} \text{ cm}^{-1}$) [see Fig. 4, trace (b)] which can be assigned to d-d transitions of Ni^I in a planar or axially distorted geometry.^{31–33} In Fig. 4 is also given the spectrum of **2** for comparison [trace (a)]. For isoelectronic copper(II) complexes of *N,N'*-bis(salicylidene)ethane-1,2-diamine (H₂salen) and related ligands the three d-d transitions are close in energy and appear as a superposed band as discussed above. This arises from a signifi-

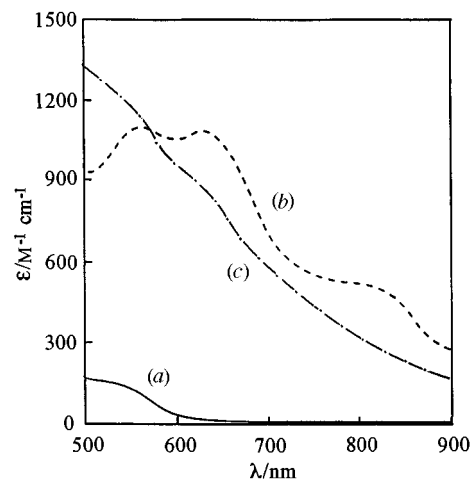


Fig. 4 Visible spectra of (a) complex **2**, (b) its Ni^ICo^{II} complex and (c) the Ni^ICo^I complex in dmsO

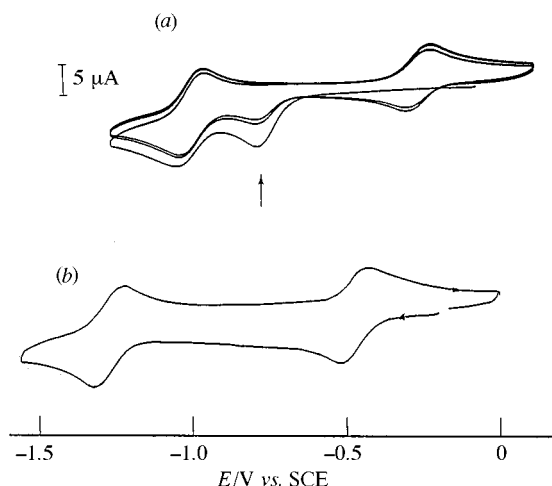
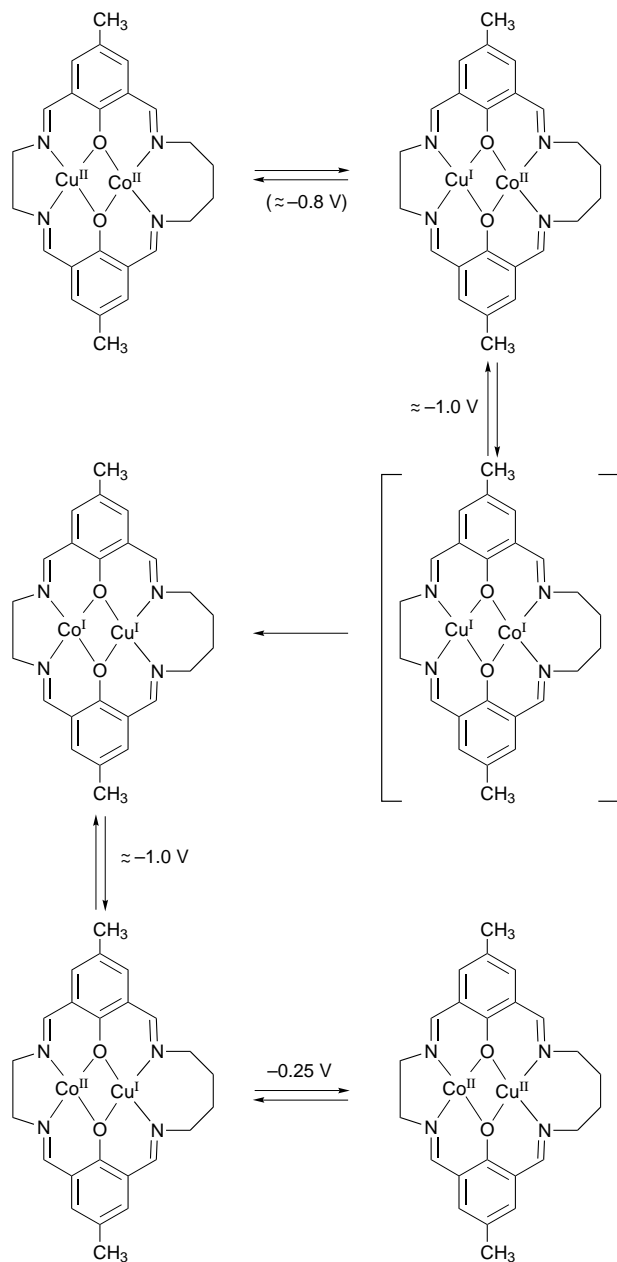


Fig. 5 Cyclic voltammograms of complexes **4** (a) and **5** (b). Conditions: glassy-carbon electrode, scan rate 50 mV s⁻¹, concentration of 1 × 10⁻³ M, in dmsO

cant antibonding nature of the metal d_{yz} and d_{zx} orbitals^{34,35} giving the d-orbital ordering d_{x²-y²} > d_{z²} ≈ d_{xz}, d_{yz} ≈ d_{xy}. In the Ni^ICo^{II} complex the antibonding nature of the d_{xz} and d_{yz} orbitals must be enhanced because the bridging phenolic oxygens have a sp² hybridization character and Ni^I has a larger ionic radius, leading to the separation of d orbitals in the order d_{x²-y²} > d_{xz}, d_{yz} > d_{z²} > d_{xy}. Thus, the three absorptions found for this complex can be assigned to the d_{xy} → d_{x²-y²}, d_{z²} → d_{x²-y²} and d_{xz}, d_{yz} → d_{x²-y²} transitions from shorter wavelength. The complex is ESR-silent at liquid-nitrogen temperature, probably because of antiferromagnetic interaction between the nickel(I) and cobalt(II) ions as inferred from the isoelectronic Cu^{II}Co^{II} complexes **3–5** discussed above.

The second wave at lower potential is attributed to reduction of the cobalt(II) centre to give a Ni^ICo^I species, based on the coulometry of **2** at -1.40 V. The electrolysed solution is red and shows two absorptions at 550 (1100) and 630 nm ($\epsilon = 700 \text{ M}^{-1} \text{ cm}^{-1}$) [Fig. 4, trace (c)]. The visible spectral features observed for the Ni^ICo^{II} complex do not persist in the spectrum of the Ni^ICo^I complex. This fact implies that the reduction at the cobalt(II) centre gives rise to a change in the NiCo core structure so that the electronic nature of the Ni^I is altered. Both the Ni^ICo^{II} and Ni^ICo^I complexes are sensitive to molecular oxygen and reoxidized to the Ni^{II}Co^{II} complex when exposed to air.

It is noticeable that the second process Ni^ICo^{II} → Ni^ICo^I occurs at a high potential in complex **1** (-1.25 V) relative to **2**



Scheme 1 Site exchange of metal ions in complex **4** at the electrode

(-1.44 V). This may reflect the geometric surrounding about the cobalt ion in each complex. That is, the CoN_2O_2 chromophore of **1**, comprised of the trimethylene chain, can adopt a planar geometry preferred for Co^{I} (d^8). On the other hand, the CoN_2O_2 chromophore of **2**, comprised of a tetramethylene chain, cannot adopt such a planar geometry, making difficult the reduction of $\text{Ni}^{\text{I}}\text{Co}^{\text{II}}$ to $\text{Ni}^{\text{I}}\text{Co}^{\text{I}}$.

The cyclic voltammogram of the CuCo complex **3** showed ill resolved waves and varied complicatedly with the repeat of the sweep. It appears that **3** is unstable at the electrode, resulting in scrambling of metal ions.

The cyclic voltammogram of complex **4** is given in Fig. 5 (a). In the first sweep to negative potential it showed a cathodic peak near -0.8 V and a quasi-reversible couple near -1.0 V. In the return of the sweep no anodic peak corresponding to the cathodic peak near -0.8 V appeared. Instead, a new couple appeared at -0.25 V. With the repeat of sweep the cathodic wave near -0.8 V diminished its intensity, finally giving two quasi-reversible couples at -0.25 and -1.0 V. The couple at -0.25 V did not appear in the sweep in the potential range of 0 to -0.9 V. The electrochemical feature observed suggests a core structural change when reduced to $\text{Cu}^{\text{I}}\text{Co}^{\text{I}}$.

It must be pointed out that dinuclear copper(II) complexes of

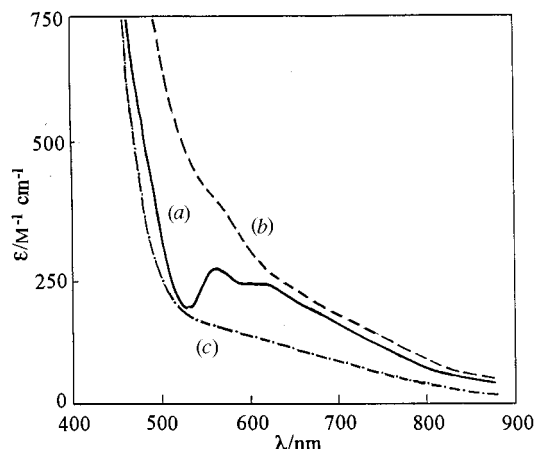


Fig. 6 Visible spectra of (a) complex **5**, (b) its $\text{Cu}^{\text{I}}\text{Co}^{\text{II}}$ complex and (c) the $\text{Cu}^{\text{I}}\text{Co}^{\text{I}}$ complex in dmsO

analogous macrocycles having a tetramethylene lateral chain show the first reduction wave at higher potential (≈ -0.3 V).^{36,37} This fact strongly suggests that the Cu in **4** moves from the site of the ethylene lateral chain to the site of the tetramethylene chain at the electrode. Based on this presumption the cathodic wave near -0.8 V observed in the first sweep can be attributed to the reduction of the Cu^{II} at the site of the ethylene lateral chain and the couple near -1.0 V to the $\text{Co}^{\text{II}} \rightarrow \text{Co}^{\text{I}}$ process at the site of the tetramethylene chain. In the resulting $\text{Cu}^{\text{I}}\text{Co}^{\text{I}}$ complex, Cu^{I} of d^{10} electronic configuration prefers a non-planar geometry and Co^{I} of d^8 electronic configuration a planar geometry when it assumes low spin. Thus, site exchange of the metal ions may occur forming a coordination-position isomer possessing Co at the site of the ethylene lateral chain and Cu at the site of the tetramethylene chain (see Scheme 1). It appears that the $\text{Co}^{\text{II}} \rightarrow \text{Co}^{\text{I}}$ process of the high-spin Co^{II} at the site of the tetramethylene lateral chain and that of the low-spin Co^{II} at the site of the ethylene lateral chain occur at similar potential by chance.

Complex **5** has two quasi-reversible couples at -0.48 and -1.27 V both of which show good stability upon repeating the sweep at the electrode [see Fig. 5 (b)]. Controlled-potential electrolyses have demonstrated one-electron transfer at -0.5 V and two-electron transfer at -1.2 V. Thus, the two couples can be assigned to the stepwise redox processes $\text{Cu}^{\text{II}}\text{Co}^{\text{II}} \rightarrow \text{Cu}^{\text{I}}\text{Co}^{\text{II}}$ and $\text{Cu}^{\text{I}}\text{Co}^{\text{II}} \rightarrow \text{Cu}^{\text{I}}\text{Co}^{\text{I}}$, respectively. The solution of the $\text{Cu}^{\text{I}}\text{Co}^{\text{II}}$ complex is yellow and shows two absorptions around 560 and 700 nm which are assigned to the cobalt(II) ion [Fig. 6, trace (b)]. The two bands are apparently enhanced due to the superposition on a near-UV band occurring around 430 nm. It must be pointed out that the $\text{Cu}^{\text{I}}\text{Mn}^{\text{II}}$ complex of $(\text{L}^{2,3})^{2-}$ also has a similar near-UV band around 430 nm.²⁹ When we subtract the tailing of the near-UV band, an absorption coefficient of *ca.* $50 \text{ M}^{-1} \text{ cm}^{-1}$ at best is evaluated for the bands at ≈ 560 and ≈ 700 nm. These bands are evidently weak compared with the two visible bands at 560 and 620 nm of **5** [trace (a)], leading to the conclusion that the two visible bands of **5** originate from the copper(II) ion. The $\text{Cu}^{\text{I}}\text{Co}^{\text{I}}$ complex is brown and its visible spectrum [trace (c)] suggests the presence of some absorption bands in the region 500–700 nm.

Based on the above studies it is shown that rare $\text{Ni}^{\text{I}}\text{Co}^{\text{I}}$ complexes can be produced using $(\text{L}^{2,3})^{2-}$ and $(\text{L}^{2,4})^{2-}$ and a $\text{Cu}^{\text{I}}\text{Co}^{\text{I}}$ complex using $(\text{L}^{3,3})^{2-}$ in bulk solution, though the spin state of the Co^{I} in each complex remains to be clarified.

Acknowledgements

This work was supported by a Grant-in-Aid for Scientific Research (No. 09440231) from the Ministry of Education, Science and Culture, Japan.

References

- 1 O. Kahn, *Struct. Bonding (Berlin)*, 1987, **68**, 89.
- 2 P. Zanello, S. Tamburini, P. A. Vigato and G. A. Mazzocchin, *Coord. Chem. Rev.*, 1987, **77**, 165.
- 3 P. A. Vigato, S. Tamburini and D. E. Fenton, *Coord. Chem. Rev.*, 1990, **106**, 25.
- 4 N. Sträter, T. Klabunde, P. Tucker, H. Witzel and B. Krebs, *Science*, 1995, **268**, 1489.
- 5 C. R. Kissinger, H. E. Parge, D. R. Knighton, C. T. Lewis, L. A. Pelletier, A. Tempczyk, V. J. Kalish, K. D. Tucker, R. E. Showalter, E. W. Moomaw, L. N. Gastinel, N. Habuka, X. Chen, F. Maldonado, J. E. Barker, R. Bacquet and J. E. Villafranca, *Nature (London)*, 1995, **378**, 641.
- 6 M.-P. Egloff, P. T. W. Cohen, P. Reinemer and D. Barford, *J. Mol. Biol.*, 1995, **254**, 942.
- 7 D. E. Fenton and H. Okawa, *Chem. Ber.*, 1997, **130**, 433.
- 8 H. Okawa and S. Kida, *Inorg. Nucl. Chem. Lett.*, 1971, **7**, 751; *Bull. Chem. Soc. Jpn.*, 1972, **45**, 1759.
- 9 M. Tadokoro, H. Okawa, N. Matsumoto, M. Koikawa and S. Kida, *J. Chem. Soc., Dalton Trans.*, 1991, 1657; M. Tadokoro, H. Sakiyama, N. Matsumoto, M. Kodaera, H. Okawa and S. Kida, *J. Chem. Soc., Dalton Trans.*, 1992, 313.
- 10 H. Okawa, J. Nishio, M. Ohba, M. Tadokoro, N. Matsumoto, M. Koikawa, S. Kida and D. E. Fenton, *Inorg. Chem.*, 1993, **32**, 2949; J. Nishio, H. Okawa, S. Ohtsuka and M. Tomono, *Inorg. Chim. Acta*, 1994, **218**, 27; J. Shimoda, H. Furutachi, M. Yonemura, M. Ohba, N. Matsumoto and H. Okawa, *Chem. Lett.*, 1996, 979.
- 11 S. Ohtsuka, M. Kodaera, K. Motoda, M. Ohba and H. Okawa, *J. Chem. Soc., Dalton Trans.*, 1995, 2599.
- 12 M. Yonemura, Y. Matsumura, M. Ohba, H. Okawa and D. E. Fenton, *Chem. Lett.*, 1996, 601.
- 13 C. Fraser, S. L. Johnston, A. L. Rheingold, B. S. Haggerty, G. K. Williams, J. Whelan and B. Bosnich, *Inorg. Chem.*, 1992, **31**, 1835; D. G. McCollum, G. P. A. Yap, A. L. Rheingold and B. Bosnich, *J. Am. Chem. Soc.*, 1996, **118**, 1365 and refs. therein.
- 14 S. Karunakaran and M. Kandaswamy, *J. Chem. Soc., Dalton Trans.*, 1994, 1595.
- 15 N. H. Pilkington and R. Robson, *Aust. J. Chem.*, 1970, **23**, 2225; B. F. Hoskins, R. Robson and G. A. Williams, *Aust. J. Chem.*, 1975, **28**, 2598; *Inorg. Chim. Acta*, 1975, **29**, 2607; 1976, **16**, 16, 121.
- 16 N. F. Curtis, *J. Chem. Soc.*, 1961, 3147.
- 17 E. A. Boudreaux and L. N. Mulay, *Theory and Applications of Molecular Paramagnetism*, Wiley, New York, 1976, pp. 491–494.
- 18 D. A. Denton and H. Suschitzky, *J. Chem. Soc.*, 1963, 4741.
- 19 D. T. Cromer and J. T. Waber, *International Tables for X-Ray Crystallography*, Kynoch Press, Birmingham, 1974, vol. 4.
- 20 D. C. Creagh and W. J. McAuley, in *International Tables for Crystallography*, Kluwer, Boston, 1992, vol. C.
- 21 D. C. Creagh and H. H. Hubbell, in *International Tables for Crystallography*, Kluwer, Boston, 1992, vol. C.
- 22 TEXSAN, Molecular Structure Corporation, Houston, TX, 1985.
- 23 R. R. Gagne, C. L. Spiro, T. J. Smith, C. A. Hamann, W. R. Thies and A. K. Shiemke, *J. Am. Chem. Soc.*, 1981, **103**, 4073.
- 24 B. V. Crook, H. Doine, F. F. Stephens, M. J. Cannon and R. D. Cannon, *Polyhedron*, 1989, **8**, 2007.
- 25 B. Bosnich, *J. Am. Chem. Soc.*, 1968, **90**, 627.
- 26 R. S. Downing and F. L. Urbach, *J. Am. Chem. Soc.*, 1968, **90**, 627.
- 27 S. M. Crawford, *Spectrochim. Acta*, 1963, **19**, 225.
- 28 C. K. Johnson, ORTEP, Report 3794, Oak Ridge National Laboratory, Oak Ridge, TN, 1965.
- 29 H. Wada, T. Aono, K. Motoda, M. Ohba, N. Matsumoto and H. Okawa, *Inorg. Chim. Acta*, 1996, **246**, 13.
- 30 H. Wada, K. Motoda, M. Ohba, H. Sakiyama, N. Matsumoto and H. Okawa, *Bull. Chem. Soc. Jpn.*, 1995, **68**, 1105.
- 31 M. P. Sue, H. K. Kim, M. J. Kim and K. Y. Oh, *Inorg. Chem.*, 1992, **31**, 3620.
- 32 H. Okawa, Y. Aratake, K. Motoda, M. Ohba, H. Sakiyama and N. Matsumoto, *J. Supramol. Chem.*, 1996, **6**, 293.
- 33 H. Wada, T. Aono, K. Motoda, M. Ohba, N. Matsumoto and H. Okawa, *Inorg. Chim. Acta*, 1996, **246**, 13.
- 34 H. Okawa and D. H. Busch, *Inorg. Chem.*, 1979, **18**, 1555.
- 35 Y. Nishida and S. Kida, *Coord. Chem. Rev.*, 1979, **27**, 275.
- 36 R. C. Long and D. N. Hendrickson, *J. Am. Chem. Soc.*, 1983, **105**, 1513.
- 37 A. W. Addison, *Inorg. Nucl. Chem. Lett.*, 1976, 12, 899.

Received 2nd April 1997; Paper 7/02210G